A modified TV-Stokes model for image processing

William G. Litvinov, Talal Rahman, Xue-Cheng Tai

Angaben zur Veröffentlichung / Publication details:

Litvinov, William G., Talal Rahman, and Xue-Cheng Tai. 2009. "A modified TV-Stokes model for image processing." Augsburg: Universität Augsburg.

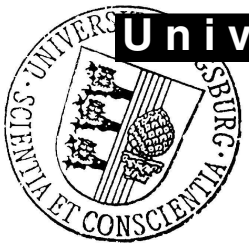

Universität Augsburg

Institut für
Mathematik

William G. Litvinov, Talal Rahman, Xue-Cheng Tai

A Modified TV-Stokes Model for Image Processing

Preprint Nr. 25/2009 — 14. Oktober 2009
Institut für Mathematik, Universitätsstraße, D-86135 Augsburg http://www.math.uni-augsburg.de/

Impressum:

Herausgeber:

Institut für Mathematik
Universität Augsburg
86135 Augsburg
`http://www.math.uni-augsburg.de/pages/de/forschung/preprints.shtml`

ViSdP:

William G. Litvinov
Institut für Mathematik
Universität Augsburg
86135 Augsburg

A MODIFIED TV-STOKES MODEL FOR IMAGE PROCESSING

WILLIAM G. LITVINOV *, TALAL RAHMAN †, AND XUE-CHENG TAI ‡

Abstract. We introduce and investigate the modified TV-Stokes model for two classical image processing tasks, i.e., image restoration and image inpainting. The modified TV-Stokes model is a two-step model based on a total variation (TV) minimization in each step and the use of geometric information of the image. In the first step, a smoothed and divergence free tangential field of the given image is recovered, and in the second step, the image is reconstructed from the corresponding normals. The existence and the uniqueness of the solution to the minimization problems are established for both steps of the model. Numerical examples and comparisons are presented to illustrate the effectiveness of the model.

Key words. Total Variation, image restoration, image inpainting

image restoration **AMS subject classifications.** 65F10, 65N30, 65N55

1. Introduction. Variational models based on two minimizing steps or a two-step approach have recently been adapted to image processing, cf. [28, 33, 35, 9, 22]. Until now there has not been any theoretical analysis of such models, in many cases they do not generate well-posed problems. In this paper, we reformulate the ideas mentioned in the earlier papers, and propose a new variant of the two-step model which leads to a correct problem that has a unique solution.

We consider the problem of inpainting an image in areas where information may be missing, or denoising an image which may contain some additive noise. In either cases, we are given an image $y : \Omega \to \mathbb{R}$ which is the gray intensity of the image, and Ω is a bounded domain in $\mathbb{R}^2$ with a Lipschitz continuous boundary, e.g. a rectangular domain for an image.

In case of denoising, we have

$$y = h + \eta,$$

where h is the true image and η is the noise. In case of inpainting, the area of missing information, also known as the inpainting region, is denoted by Ω_I. Consequently,

$$y|_{\Omega\setminus\Omega_I} = h|_{\Omega\setminus\Omega_I}. \tag{1.1}$$

One of the earliest models for image denoising, based on variational calculus, is the classical second order model due to Rudin, Osher and Fatemi [32]:

$$\min_{h\in BV(\Omega)} \left\{ E_{ROF}(h) = \int_\Omega |Dh| \; dx + \frac{\mu}{2}\int_\Omega (y-h)^2 \; dx \right\}, \tag{1.2}$$

referred to as the ROF model. Here one looks for a minimizer u in the space $BV(\Omega)$ of functions from $L^1(\Omega)$ with bounded total variation $TV(h) = \int_\Omega |Dh|dx < \infty$ defined

*Department of Mathematics, University of Augsburg, Universitätstr. 14, 86159 Augsburg, Germany (Email: litvinov@math.uni-augsburg.de).

†Center for Integrated Petroleum Research, c/o Department of Mathematics, University of Bergen, Johannes Brunsgate. 12, 5008 Bergen, Norway (Email: talal.rahman@math.uib.no).

‡Department of Mathematics, University of Bergen, c/o Center for Integrated Petroleum Research, Allégt. 41, 5007 Bergen,Norway (Email: tai@math.uib.no).

as

$$\int_\Omega |Dh|\ dx = \sup_p \int_\Omega h \ \text{div}\ p\ dx, \tag{1.3}$$
$$p = (p_1, p_2) \in C_0^1(\Omega; \mathbb{R}^2), \quad |p_i(x)| \le 1, \quad x \in \Omega, \quad i = 1, 2.$$

The model has a unique solution in BV, cf. [14], and it is well known for preserving edges in an image. However, since the model favors step functions the resulting image gets a staircase effect in the smooth regions. Generally, total variation is a very simple descriptor of image.

Many more advanced models were developed, which take into account the values of the observed image. These are models founded on l^1 norms, on wavelet, nonlocal models, and others. Profound review of such image denoising models is contained in [8], see also [11], [12].

In order to take into account not only the values of the observed image, but also the values of the derivatives of it, and to suppress the staircase effect, a number of fourth order models have been developed, cf. [16, 27, 37]. These models are based on minimization of the total variation of the derivatives of the restored image and the total variation of the image itself. In addition, here the function of the observed image and its derivatives are approximated in the norm of the space $L_2(\Omega)$. Existence and uniqueness result for the fourth order model due to Lundervold-Lysaker-Tai (LLT) [27] can be found in [26]. However, problems with high order derivatives are inconvenient for numerical solution, see e.g. [13]. In addition, it has also been observed that images produced by some fourth order problems, cf. [27], may still look patchy in smooth regions.

Instead of having to deal with a fourth order model, the two-step models have started to appear as an efficient tool for image denoising, cf. [9, 28, 33, 35]. The basic approach in a two-step model is, to reduce the fourth order problem to two second order problems.

Among the early two-step models is the one due to Burchard, Tasdizen, Whitaker and Osher, cf. [9], for processing deformable surfaces via level set method.

This idea was further extended to image processing in [28] by Lysaker, Osher and Tai (LOT). Here in the first step, one seeks a function of directions of gradients $n^0 = (n_1^0, n_2^0)$ that is the solution of the following problem:

$$E^1(n^0) = \min_{|n| \le 1} E^1(n), \tag{1.4}$$

$$E^1(n) = \int_\Omega |Dn|\ dx + \frac{\delta}{2} \int_\Omega \left(n - \frac{\nabla y}{|\nabla y|} \right)^2\ dx. \tag{1.5}$$

In the second step, the image function h_0 is reconstructed as the solution of the following minimization problem:

$$E^2(h_0) = \min_h E^2(h), \tag{1.6}$$

$$E^2(h) = \int_\Omega \left(|Dh| - n^0 \cdot Dh \right)\ dx + \frac{\mu}{2} \int_\Omega (y - h)^2\ dx. \tag{1.7}$$

Numerical calculations show that this model preserves the edges comparatively much better than the ROF and the fourth order models.

However, the functional $E^2(h)$ has no sense in the space $BV(\Omega)$, if n^0 does not possess some smoothness.

Another two-step model has been used in [35] for inpainting, and later in [33] for denoising. Here the first minimization step of the LOT model is replaced by the following minimization problem:

$$\min\left\{E^3(u)=\int_\Omega |Du|\ dx+\frac{\delta}{2}\int_\Omega \left(u-\nabla^\perp y\right)^2\ dx\right\},\quad \operatorname{div} u=0. \tag{1.8}$$

Here $\nabla^\perp y=(-\frac{\partial y}{\partial x_2},\frac{\partial y}{\partial x_1})$ is the function of tangential vectors that are orthogonal to the vectors of normals to the image surface $\nabla y=(\frac{\partial y}{\partial x_1},\frac{\partial y}{\partial x_2})$. The constraint $\operatorname{div} u=0$ follows from the fact that $\operatorname{div}\nabla^\perp \mathrm{y}=0$.

Once the solution of the problem (1.8) is known, the corresponding function of normal vectors is defined and the problem (1.6) is solved in the second step.

The resulting model, known as the TV-Stokes model preserves edges in an image and at the same time produce smooth surfaces. However, as indicated above, the functional E^2 from (1.7) has no sense in the space $BV(\Omega)$ if n^0 is not smooth.

Below, we replace the functional E^2 by a new one and consider a two-step model in which the problem (1.8) is solved in the first step and a minimization problem for a new functional is solved in the second step. We call the new two-step model as the modified TV-Stokes model. This model is introduced in Section 2 and in Section 3, we study it and its regularization. Results on the existence and the uniqueness of the solution for the first and the second steps for the original and the regularized models are proved. It is also argued that solutions of the regularized problems converge to the solutions of the initial problems for the first and the second steps as the parameter of regularization tends to zero. In Sections 4 and 5, the algorithm and numerical results are presented

2. The modified TV-Stokes model. The image h can be considered as a surface. The normal and the tangential vectors to the surface are given by $n=\nabla h(x)=(h_{x_1},h_{x_2})$ and $u=\nabla^\perp h=(-h_{x_2},h_{x_1})$. The vector fields then satisfy the following conditions: $\operatorname{div} u=0$ and $\nabla\times n=0$, the first one being called the incompressibility condition in fluid mechanics.

Let the noisy image y be given. We suppose that $y\in H^1(\Omega)$.

The noisy image is obtained by approximation of a discrete grid of samples. The Shannon interpolation of the discrete grid is usually used, see [8], [34]. Then the function y is analytic. The function y can also be obtained by the piecewise affine approximation. Then $y\in H^1(\Omega)$. Hence, the assumption that y belongs to $H^1(\Omega)$.is not restrictive.

We compute the tangential field $v=\nabla^\perp y$. The algorithm is then defined in two steps. In the first step, we solve the following minimization problem:

$$\min\left\{\int_\Omega \left(|Du_1|+|Du_2|\right)dx\ +\ \frac{\delta}{2}\int_\Omega\sum_{i=1}^{2}(u_i-v_i)^2dx\right\},$$
$$u\in BV(\Omega;\mathbb{R}^2),\ \operatorname{div} u=0. \tag{2.1}$$

Here δ is a positive parameter which is used to get a balance between the smoothing of the tangent field and the fidelity to the noisy tangent field. The constraint $\operatorname{div} u=0$ is understood in the sense of distribution. This constraint inserts the coupling between u_1 and u_2.

Let $u^0=(u_1^0,u_2^0)$ be the solution to the problem (2.1), i.e., u^0 is the smoothed tangent field. The corresponding normal field is $n^0=(u_2^0,-u_1^0)$.

In the second step, we reconstruct our image by fitting it to the normal field and the values of y of the noisy image. Here we solve the following minimization problem:

$$\min_{h\in BV(\Omega)} \left\{ \int_\Omega \left| Dh - n^0 \right| dx + \frac{\mu}{2} \int_\Omega (y-h)^2 \, dx \right\}, \tag{2.2}$$

where μ is a positive parameter. The parameter μ is defined by the noise level σ that is given as $\sigma^2 = \int_\Omega \eta^2 \, dx$. This value is estimated by using statistical methods. A large value of μ would result in under-smoothing, and a small value in over-smoothing.

3. Investigation of the model.

3.1. Tangent field smoothing.

We define a functional J as follows:

$$J(u) = \int_\Omega (|Du_1| + |Du_2|) \, dx + \frac{\delta}{2} \int_B \sum_{i=1}^{2} (u_i - v_i)^2 dx. \tag{3.1}$$

Here v is a given function,

$$v = (v_1, v_2) \in L_2(B; \mathbb{R}^2), \tag{3.2}$$

and $B \subset \Omega$ is a subdomain with Lipschitz continuous boundary. We consider $B = \Omega$ in the case of denoising and $B = \Omega \setminus \Omega_I$ in the case of inpainting. The terms $\int_\Omega |Du_i| \, dx$, $i = 1, 2$, are defined by (1.3).

We will prove the following result:

THEOREM 3.1. *Let Ω be a bounded domain in $\mathbb{R}^2$ with a Lipschitz continuous boundary S. Let also B be a subdomain of Ω with a Lipschitz continuous boundary Λ, in particular, it can be $B = \Omega$. Then the expression*

$$\| u \|_{BV(\Omega;\mathbb{R}^2)} = \int_\Omega (|Du_1| + |Du_2|) \, dx + \left(\int_B |u|^2 \, dx \right)^{\frac{1}{2}}, \tag{3.3}$$

where $|u|^2 = u_1^2 + u_2^2$, defines a norm in $BV(\Omega; \mathbb{R}^2)$ that is equivalent to the following main norm of $BV(\Omega; \mathbb{R}^2)$:

$$\| u \|_1 = \int_\Omega (|Du_1| + |Du_2| + |u_1| + |u_2|) \, dx. \tag{3.4}$$

The proof of this theorem is given in Section 3.3.

Let us consider the problem: Find u^0 such that

$$u^0 \in U, \quad J(u^0) = \inf_{u\in U} J(u), \tag{3.5}$$

where

$$U = \{u |\ u = (u_1, u_2) \in BV(\Omega; \mathbb{R}^2),\ \text{div } u = 0\}. \tag{3.6}$$

For a function $u \in BV(\Omega; \mathbb{R}^2)$, the condition div $u = 0$ can be rewritten as follows:

$$\int_\Omega \left(u_1 \frac{\partial \xi}{\partial x_1} + u_2 \frac{\partial \xi}{\partial x_2} \right) dx = 0, \ \xi \in C_0^1(\Omega).$$

By using the embedding theorem in BV (cf. [1], p.152), it is easy to check that U is a closed subspace in $BV(\Omega;\mathbb{R}^2)$, i.e. U is a Banach space with the norm (3.3) or (3.4).

THEOREM 3.2. *Suppose that Ω is a bounded domain in $\mathbb{R}^2$ with a Lipschitz continuous boundary S, and let also (3.2) holds. Then there exists a unique solution of the problem (3.5).*

Proof. Let $\{u^j\}$ be a minimizing sequence, i. e.

$$\{u^j\} \subset U,\ \lim J(u^j) = \inf_{u\in U} J(u). \tag{3.7}$$

It follows from (3.1) and (3.3) that the sequence $\{u^j\}$ is bounded in $BV(\Omega;\mathbb{R}^2)$. Therefore, a subsequence $\{u^k\}$ can be extracted such that

$$u^k \rightharpoonup u^0 \text{ in } BV(\Omega;\mathbb{R}^2), \tag{3.8}$$

and

$$u^k \to u^0 \text{ in } L_p(\Omega;\mathbb{R}^2) \ \text{ for } p<2, \quad u^k \rightharpoonup u^0 \text{ in } L_2(\Omega;\mathbb{R}^2), \tag{3.9}$$

where $\rightharpoonup$ denotes the weak convergence (see [1], Theorem 3.23, p. 132, [3], p. 40, 41).

It follows from (3.9) that div $u^0 = 0$ and, hence, $u^0 \in U$. (3.8) and (3.9) imply

$$\liminf_{k\to\infty} J(u^k) \geq J(u^0).$$

Therefore, u^0 is a solution of the problem (3.5).

The functional $u \to \| u\|^2$ is strictly convex. Therefore, the functionals ψ and J are strictly convex, and there exists a unique function u^0 such that (3.5) holds. Because of this, (3.8) and (3.9) are valid not only for the subsequence $\{u^k\}$, but for the sequence $\{u^j\}$ as well. $\diamond$

We introduce the following regularization J_α of the functional J:

$$J_\alpha(u) = \int_\Omega \left(\sqrt{\alpha^2+|Du_1|^2} + \sqrt{\alpha^2+|Du_2|^2}\right)\, dx + \frac{\delta}{2}\int_B \sum_{i=1}^{2}(u_i - v_i)^2\, dx. \tag{3.10}$$

Here α is a small positive number, and the first term is defined by the following relation (see [2]):

$$\int_\Omega \sqrt{\alpha^2+|Du_i|^2}\, dx = \sup_p \Big\{\int_\Omega (-u_i \text{ div } p + \sqrt{\alpha^2(1-p^2)}\,)\, dx\Big\}, \tag{3.11}$$
$$p=(p_1,p_2)\in C_0^1(\Omega;\mathbb{R}^2),\ |p_k(x)|\leq 1,\ x\in\Omega,\ k=1,2\Big\}.$$

We consider the problem: Find u^α such that

$$u^\alpha \in U, \quad J_\alpha(u^\alpha) = \inf_{u\in U} J_\alpha(u). \tag{3.12}$$

The computational advantage of the functional J_α over the functional J is that it is differentiable when ∇u_i vanish in Ω. The set of infinitely differentiable in $\overline{\Omega}$ functions is dense in $BV(\Omega)$. Taking into account that the operator of regularization, which is defined by a mollifier, is permutable with the operator of differentiation, see e.g. [19], Section 14, one can ensure, that the set of infinitely differentiable in $\overline{\Omega}$ vector functions v satisfying the condition div $u = 0$ is dense in U.

The functional J_α is infinitely differentiable in $U \cap C^\infty(\overline{\Omega};\mathbb{R}^2)$. Because of this one can use effective numerical methods for approximate solution of the problem (3.12).

THEOREM 3.3. *Suppose that Ω is a bounded domain in $\mathbb{R}^2$ with a Lipschitz continuous boundary S, and let (3.2) hold. Then for an arbitrary $\alpha > 0$, there exists a unique solution u^α to problem (3.12). If $u^\alpha \in W_1^1(\Omega;\mathbb{R}^2)$, then the following condition is satisfied:*

$$(J'_\alpha(u^\alpha), h) = \int_\Omega (\alpha^2 + |\nabla u_i^\alpha|^2)^{-\frac{1}{2}} \frac{\partial u_i^\alpha}{\partial x_j} \frac{\partial h_i}{\partial x_j}\, dx + \delta \int_B (u_i^\alpha - v_i) h_i\, dx = 0, \qquad (3.13)$$

where $h \in W_1^1(\Omega;\mathbb{R}^2)$, $\operatorname{div} \mathrm{h} = 0$.

Indeed, the functional J_α is growing and strictly convex. Therefore, there exists a unique solution of the problem (3.12). If $u^\alpha \in W_1^1(\Omega;\mathbb{R}^2)$, then (3.13) holds.

We mention that in (3.13) and below the Einstein convention on summation over repeated index is applied.

THEOREM 3.4. *Let Ω be a bounded domain in $\mathbb{R}^2$ with a Lipschitz continuous boundary S, and let also (3.2) hold. Then*

$$u^\alpha \to u^0 \text{ in } L_p(\Omega;\mathbb{R}^2) \quad \text{at} \quad p < 2, \quad u^\alpha \rightharpoonup u^0 \text{ in } BV(\Omega;\mathbb{R}^2) \quad \text{as } \alpha \to 0, \qquad (3.14)$$

where u^α and u^0 are the solutions of the problems (3.12) and (3.5), respectively.

Proof. It follows from (3.11) that

$$\int_\Omega \sqrt{\alpha^2 + |Du_i|^2}\, dx \le \int_\Omega \sqrt{|Du_i|^2}\, dx + \alpha|\Omega|,$$

where $|\Omega| = \int_\Omega dx$. Therefore,

$$|J(u) - J_\alpha(u)| \le \alpha|\Omega|. \qquad (3.15)$$

Obviously

$$J_\alpha(u) \to \infty \quad \text{as} \quad \| u \|_{BV(\Omega;\mathbb{R}^2)} \to \infty, \quad \alpha \in [0, \alpha_0]. \qquad (3.16)$$

Taking (3.12), (3.15), and (3.16) into account, we obtain,

$$\| u^\alpha \|_{BV(\Omega;\mathbb{R}^2)} \le C \qquad (3.17)$$

for all $\alpha \in (0, \alpha_0]$. Thus, we can extract a subsequence, which is still denoted $\{u^\alpha\}$, such that

$$u^\alpha \rightharpoonup z \text{ in } BV(\Omega;\mathbb{R}^2) \text{ as } \alpha \to 0. \qquad (3.18)$$

It follows from here that

$$z \in U. \qquad (3.19)$$

Relations (3.18) and (3.15) yield

$$J(z) \le \liminf J(u^\alpha) = \liminf J_\alpha(u^\alpha). \qquad (3.20)$$

(3.12) and (3.15) imply

$$\liminf J_\alpha(u^\alpha) = \inf_{u \in U} J(u) \quad \text{as } \alpha \to 0. \qquad (3.21)$$

From (3.19)–(3.21) it follows that the function $u^0 = z$ is the solution of the problem (3.5). Since the problem (3.5) has unique solution, the relation (3.14) is true for an arbitrary sequence $\{u^\alpha\}$ such that $\alpha \to 0$. $\diamond$

3.2. Image reconstruction. Let $u^0 = (u_1^0, u_2^0) \in U$ be the solution of the problem (3.5), where U is defined by (3.6). We consider the second step reconstruction of the image function h. Since $\operatorname{div} u^0 = 0$, there exists a function g such that

$$u_1^0 = \frac{\partial g}{\partial x_2} \quad \text{and} \quad u_2^0 = -\frac{\partial g}{\partial x_1}, \tag{3.22}$$

(see [18] Chapter 1, Theorem 3.1).

Here we assume that Ω is a simply-connected domain. In the case that Ω is a multi-connected domain, the following additional condition should be satisfied

$$\int_{S_i} u_\nu^0 ds = 0, \quad i = 1, ..., k, \tag{3.23}$$

where u_ν^0 is the normal component of the vector u^0 and S_i are connected components of the boundary S of Ω. Since u_1^0 and u_2^0 belong to $L_2(\Omega)$ (embedding of $BV(\Omega)$ in $L_2(\Omega)$ is continuous for $n = 2$), the function g is an element of $H^1(\Omega)$, and it is defined with an accuracy of a constant addend.

It follows from (3.22) that

$$\nabla g = \left(\frac{\partial g}{\partial x_1}, \frac{\partial g}{\partial x_2} \right) = (-u_2^0, u_1^0). \tag{3.24}$$

We consider that ∇g is an approximation of ∇h. If the functions g and h are Lipschitz continuous, then the functions $u^0 = (u_1^0, u_2^0)$ and $u = (\frac{\partial h}{\partial x_2}, -\frac{\partial h}{\partial x_1})$ are tangential vectors to the level curves of the functions g and h, respectively.

The following relations hold:

$$(\nabla g, u^0) = 0, \quad (\nabla h, u) = 0. \tag{3.25}$$

We introduce the functional

$$\Psi(w) = \int_\Omega |Dw - \nabla g| \, dx + \frac{\mu}{2} \int_B (w - y)^2 \, dx. \tag{3.26}$$

Here $w \in BV(\Omega)$, $\nabla g = (-u_2^0, u_1^0)$, $y \in L_2(B)$ is a given image function, and μ is a given positive constant.

In line with the definition of the norm in $BV(\Omega)$, the first term in (3.26) is defined by

$$\int_\Omega |Dw - \nabla g| \, dx = \sup_p \int_\Omega (w - g) \operatorname{div} p \, dx, \tag{3.27}$$
$$p = (p_1, p_2) \in C_0^1(\Omega)^2, \quad |p_i(x)| \le 1, \quad x \in \Omega, \quad i = 1, 2.$$

We consider the following problem: Find h such that

$$h \in BV(\Omega), \quad \Psi(h) = \inf \Psi(w), \quad w \in BV(\Omega). \tag{3.28}$$

The solution of the problem (3.28) is regarded to be the reconstructed image.

We have considered the second step the reconstruction of the image function by the use of the function u^0 which is the solution of the problem (3.5). In similar fashion, the image function is reconstructed by the function u^α which is the solution of the

problem (3.12). In this case, the function u^0 in the above formulas is replaced by the function u^α.

THEOREM 3.5. *Suppose that Ω is a bounded domain in $\mathbb{R}^2$ with a Lipschitz continuous boundary S, and let $y \in L_2(B)$. Then there exists a unique solution of the problem (3.28).*

Proof. For $w \in BV(\Omega)$, we have,

$$\Psi(w) \geq \int_\Omega |Dw| \, dx - \int_\Omega |\nabla g| \, dx + \frac{\mu}{2} \int_B w^2 \, dx - \mu \int_B wy \, dx + \frac{\mu}{2} \int_B y^2 \, dx$$
$$\geq \int_\Omega |Dw| \, dx - \int_\Omega |\nabla g| \, dx + \frac{\mu}{2}(1-\alpha) \int_B w^2 \, dx + \frac{\mu}{2}(1 - \frac{1}{\alpha}) \int_B y^2 \, dx, \qquad (3.29)$$

where $\alpha \in (0,1)$. Therefore

$$\Psi(w) \to \infty \text{ as } \| w \|_{BV(\Omega)} \to \infty. \qquad (3.30)$$

Let $\{h_n\}$ be a minimizing sequence, that is

$$\{h_n\} \subset BV(\Omega), \quad \lim \Psi(h_n) = \inf \Psi(w), \quad w \in BV(\Omega). \qquad (3.31)$$

By (3.30), the sequence $\{h_n\}$ is bounded in $BV(\Omega)$. Because of this, there exists a subsequence $\{h_k\}$ of the sequence $\{h_n\}$, such that

$$h_k \rightharpoonup h_0 \quad \text{in } BV(\Omega), \qquad (3.32)$$
$$h_k \rightharpoonup h_0 \quad \text{in } L_2(\Omega). \qquad (3.33)$$

It follows from (3.32) and (3.33) that

$$\liminf \Psi(h_k) \geq \Psi(h_0),$$

and by virtue of (3.31), the function $h = h_0$ is the solution of the problem (3.28).

For an arbitrary $t \in [0,1]$, we have

$$\int_\Omega |tDw_1 + (1-t)Dw_2 - \nabla g| \, dx$$
$$\leq t \int_\Omega |Dw_1 - \nabla g| \, dx + (1-t) \int_\Omega |Dw_2 - \nabla g| \, dx, \quad w_1, w_2 \in BV(\Omega).$$

Therefore, the first term in the right hand side of (3.26) is a convex functional in $BV(\Omega)$. The second term is a strictly convex functional. Hence, there exists only one solution of the problem (3.28), and the theorem is proved.

We introduce the following regularization Ψ_α of Ψ:

$$\Psi_\alpha(w) = \int_\Omega (\alpha^2 + |Dw - \nabla g|^2)^{\frac{1}{2}} \, dx + \frac{\mu}{2} \int_B (w-y)^2 \, dx, \qquad (3.34)$$

where $\alpha > 0$.

Let us consider the following problem: Find h_α such that

$$h_\alpha \in BV(\Omega), \quad \Psi_\alpha(h_\alpha) = \inf \Psi_\alpha(w), \quad w \in BV(\Omega). \qquad (3.35)$$

THEOREM 3.6. *Suppose that the conditions of Theorem 3.5 are satisfied. Then for an arbitrary $\alpha > 0$ there exists a unique solution of the problem (3.35). If $h_\alpha \in W_1^1(\Omega)$, then the following condition is satisfied*

$$(\Psi'_\alpha(h_\alpha), w) = \int_\Omega (\alpha^2 + |\nabla h_\alpha - \nabla g|^2)^{-\frac{1}{2}} \left(\frac{\partial h_\alpha}{\partial x_i} - \frac{\partial g}{\partial x_i} \right) \frac{\partial w}{\partial x_i}\, dx + \mu \int_B (h_\alpha - y) w\, dx = 0, \quad w \in W_1^1(\Omega). \tag{3.36}$$

Moreover,

$$h_\alpha \rightharpoonup h \text{ in } BV(\Omega), \quad h_\alpha \rightharpoonup h \text{ in } L_2(\Omega), \qquad h_\alpha \to h \text{ in } L_p(\Omega), \quad p < 2, \quad \text{as} \quad \alpha \to 0, \tag{3.37}$$

where h is the solution of the problem (3.28)

Theorem 3.6 is proved by analogy with the proofs of theorems 3.3 and 3.4.

3.3. Proof of Theorem 3.1. Since the embedding of $BV(\Omega)$ into $L_2(\Omega)$ is continuous for $\Omega \subset \mathbb{R}^2$, we have

$$\| u \|_{BV(\Omega)^2} \le c_1 \| u \|_1, \quad u \in BV(\Omega; \mathbb{R}^2).$$

Let us establish the inverse inequality

$$\| u \|_1 \le \| u \|_{BV(\Omega;\mathbb{R}^2)}, \quad u \in BV(\Omega; \mathbb{R}^2). \tag{3.38}$$

Suppose that (3.38) is false. Then there exists a sequence $\{u^j\} \subset BV(\Omega; \mathbb{R}^2)$ such that

$$\| u^j \|_1 = 1, \quad j \in \mathbb{N}, \tag{3.39}$$

$$\int_\Omega |Du_i^j| dx \to 0 \quad \text{as} \quad j \to \infty, \quad i = 1, 2, \tag{3.40}$$

$$\int_B |u^j|^2 dx \to 0 \quad \text{as} \quad j \to \infty. \tag{3.41}$$

Therefore, a subsequence $\{u^k\}$ can be extracted that satisfies the conditions

$$u^k \rightharpoonup u^0 \quad \text{in} \quad BV(\Omega; \mathbb{R}^2), \tag{3.42}$$

$$u^k \to u^0 \quad \text{in} \quad L_p(\Omega; \mathbb{R}^2) \quad \text{for } p < 2, \tag{3.43}$$

$$u^k \rightharpoonup u^0 \quad \text{in} \quad L_2(\Omega; \mathbb{R}^2). \tag{3.44}$$

Let

$$V = \{p |\ p = (p_1, p_2) \in C_0^1(\Omega; \mathbb{R}^2), \quad p_l(x) \le 1, \quad x \in \Omega, \quad l = 1, 2\}, \tag{3.45}$$

and

$$\{p^{im}\}_{m=1}^\infty \subset V, \quad \int_\Omega |Du_i^0| dx = \lim_{m \to \infty} \int_\Omega u_i^0 \operatorname{div} p^{im} dx, \quad i = 1, 2. \tag{3.46}$$

It is evident that

$$\int_\Omega |Du_i^k| dx = \sup_{p \in V} \int_\Omega (u_i^0 + (u_i^k - u_i^0)) \operatorname{div} p\, dx. \tag{3.47}$$

We take $p = p^{im}$ in the right-hand side of (3.47). Bearing in mind (3.46), we obtain

$$\int_\Omega |Du_i^k| dx \geq \int_\Omega |Du_i^0| dx + \int_\Omega (u_i^k - u_i^0) \operatorname{div} p^{im}\, dx - \epsilon_{im}, \tag{3.48}$$
$$\epsilon_{im} > 0, \quad \lim_{m\to\infty} \epsilon_{im} = 0, \quad i = 1, 2.$$

Considering that m is fixed and granting (3.40), (3.43), we pass to the limit in (3.48) as $k \to \infty$. This gives

$$0 \geq \int_\Omega |Du_i^0| dx - \epsilon_{im},$$

that is

$$\int_\Omega |Du_i^0| dx = 0, \quad i = 1, 2. \tag{3.49}$$

Let K be an arbitrary compact set in Ω and $\overset{\circ}{K}$ be the interior of K (the interior of an arbitrary compact G is denoted by $\overset{\circ}{G}$). For sufficiently small $b > 0$, we can define in $\overset{\circ}{K}$ a function $(u_i^0)_b$ as follows:

$$(u_i^0)_b(x) = \int_{\mathbb{R}^2} \omega_b(|x - x'|) u_i^0(x')\, dx', \qquad x \in \overset{\circ}{K}, \quad i = 1, 2, \tag{3.50}$$

where

$$\omega_b \in C^\infty(\mathbb{R}_+), \quad \operatorname{supp} \omega_b \in [0, b], \quad \omega(z) \geq 0, \quad z \in \mathbb{R}_+,$$
$$\int_{\mathbb{R}^2} \omega_b(|x|)\, dx = 1. \tag{3.51}$$

The function $(u_i^0)_b$ is the regularization of u_i^0. Relations (3.50) and (3.51) yield

$$\frac{\partial (u_i^0)_b}{\partial x_k}(x) = \int_{\mathbb{R}^2} \frac{\partial \omega_b}{\partial x_k}(|x - x'|)\, u_i^0(x')\, dx'$$
$$= -\int_{\mathbb{R}^2} \frac{\partial \omega_b}{\partial x'_k}(|x - x'|)\, u_i^0(x')\, dx' = \left(\frac{\partial u_i^0}{\partial x_k}\right)_b (x), \quad x \in \overset{\circ}{K}, \quad k = 1, 2. \tag{3.52}$$

Here $\left(\frac{\partial u_i^0}{\partial x_k}\right)_b$ is the regularization of the distribution derivative $\frac{\partial u_i^0}{\partial x_k}$.

It follows from (3.49) that the partial distribution derivatives of u_i^0 are equal to zero. Because of this, (3.52) yields $\frac{\partial (u_i^0)_b}{\partial x_k}(x) = 0$ at $x \in \overset{\circ}{K}$ and, therefore,

$$(u_i^0)_b(x) = a_{ib}, \quad x \in \overset{\circ}{K}, \quad i = 1, 2, \tag{3.53}$$

where a_{1b}, a_{2b} are constants.

Since $(u_i^0)_b \to u_i^0$ in $L_2(\overset{\circ}{K})$, we obtain

$$u_i^0(x) = a_i, \quad x \in \overset{\circ}{K}, \quad i = 1, 2, \tag{3.54}$$

a_i being constants.

Let K_1 be a compact neighborhood of K such that $K_1 \subset \Omega$. Similarly to the above, we conclude that u_i^0 is defined by (3.54) in $\overset{\circ}{K}_1$ and, hence, in K_1. There exists a sequence of compact sets $\{K_j\}$ such that $K_j \subset \Omega$, $K_j \subset K_{j+1}$ for all j and $\Omega = \bigcup_{i=1}^{\infty} K_j$. Since u_i^0 is equal to a_i in every K_j, it equals a_i in Ω.

It follows from (3.41) and (3.44) that

$$\int_B |u^0|^2 \, dx = 0. \tag{3.55}$$

(3.54) and (3.55) yield

$$u^0 = (u_1^0, u_2^0) = 0. \tag{3.56}$$

Taking (3.40), (3.42), and (3.56) into account, we get

$$\lim \parallel u^k - u^0 \parallel_1 = 0. \tag{3.57}$$

Relations (3.56) and (3.57) are in contradiction with (3.39). Therefore (3.38) is valid, and the theorem is proved.

4. Algorithm. For the first step, we consider the problem (3.12) with the regularized functional J_α. It is assumed that the solution of the problem (3.12) belongs to the space $H^2(\Omega; \mathbb{R}^2)$. Apparently it will be so in the case that Ω is a regular domain and the extension of v in Ω is a smooth function. Then there exists a unique function $\lambda^\alpha \in H^1(\Omega)$ such that the pair u^α, λ^α is the unique solution of the following problem (see [4], [25], Section 6.1.3):

$$-\nabla \cdot \left(\frac{\nabla u_1^\alpha}{\sqrt{\alpha^2 + |\nabla u_1^\alpha|^2}} \right) + \delta(u_1^\alpha - v_1) + \frac{\partial \lambda^\alpha}{\partial x_1} = 0 \qquad \text{in } \Omega, \tag{4.1}$$

$$-\nabla \cdot \left(\frac{\nabla u_2^\alpha}{\sqrt{\alpha^2 + |\nabla u_2^\alpha|^2}} \right) + \delta(u_2^\alpha - v_2) + \frac{\partial \lambda^\alpha}{\partial x_2} = 0 \qquad \text{in } \Omega, \tag{4.2}$$

$$\mathrm{div} u^\alpha = 0 \qquad \text{in } \Omega, \tag{4.3}$$

$$\frac{\nabla u_1^\alpha}{\sqrt{\alpha^2 + |\nabla u_1^\alpha|^2}} \cdot \nu - \lambda^\alpha \nu_1 = 0 \quad \text{and} \quad \frac{\nabla u_2^\alpha}{\sqrt{\alpha^2 + |\nabla u_2^\alpha|^2}} \cdot \nu - \lambda^\alpha \nu_2 = 0 \quad \text{on} \quad \partial\Omega, \tag{4.4}$$

where $\nu = (\nu_1, \nu_2)$ is the unit outward normal to $\partial\Omega$ the boundary of Ω.

For the solution of the problem (4.1)-(4.4) we used the method of approximation of a solution of a stationary problem by a solution of an evolutionary problem introducing an artificial time variable t. In this case one seeks functions $u^e = (u_1^e, u_2^e), \lambda^e$, which satisfy the following conditions:

$$\frac{\partial u_1^e}{\partial t} - \nabla \cdot \left(\frac{\nabla u_1^e}{\sqrt{\alpha^2 + |\nabla u_1^e|^2}} \right) + \delta(u_1^e - v_1) + \frac{\partial \lambda^e}{\partial x_1} = 0 \quad \text{in} \quad Q = \Omega \times (0, T), \tag{4.5}$$

$$\frac{\partial u_2^e}{\partial t} - \nabla \cdot \left(\frac{\nabla u_2^e}{\sqrt{\alpha^2 + |\nabla u_2^e|^2}} \right) + \delta(u_2^e - v_1) + \frac{\partial \lambda^e}{\partial x_2} = 0 \quad \text{in} \quad Q, \tag{4.6}$$

$$\varepsilon \frac{\partial \lambda^e}{\partial t} + \mathrm{div} u^e = 0 \tag{4.7}$$

$$u^e(0) = u_0, \quad \lambda^e(0) = \lambda_0, \tag{4.8}$$

where T is a large positive constant, u_0, λ_0 are given, and $\varepsilon > 0$. In addition, the function u^e satisfies the boundary conditions (4.4) on $\Gamma = \partial\Omega \times (0,T)$, in which the index α is replaced by e.

It can be shown that the solution of a discretized evolutionary problem at an instant t converges to the solution of the discretized stationary problem as ε tends to zero and t tends to infinity; this convergence takes place for an arbitrary initial data for u^e and λ^e.

Once the function $u^\alpha = (u_1^\alpha, u_2^\alpha)$ is defined, it is used to reconstruct the image h. In this case we solve the problem (3.35) with the functional Ψ_α defined by (3.34), where $\nabla g = (-u_2^\alpha(T), u_1^\alpha(T))$, and $u_1^\alpha(T), u_2^\alpha(T)$ are the values of u_1^α, u_2^α at $t = T$. We assume that the function h_α that solves the problem (3.35) is sufficiently smooth. Then h_α is the solution of the following problem:

$$-\nabla \cdot \left(\frac{\nabla h_\alpha - \nabla g}{\sqrt{\alpha^2 + |\nabla h_\alpha - \nabla g|^2}} \right) + \mu(h_\alpha - y) = 0 \qquad \text{in } \Omega, \tag{4.9}$$

$$\left(\frac{\nabla h_\alpha - \nabla g}{\sqrt{\alpha^2 + |\nabla h_\alpha - \nabla g|^2}} \right) \cdot \nu = 0 \qquad \text{on } \partial\Omega. \tag{4.10}$$

By analogy with the above, introducing an artificial time variable t, we get the following time dependent problem, where one seeks a function h^e that satisfies the equation

$$\frac{\partial h^e}{\partial t} - \nabla \cdot \left(\frac{\nabla h^e - \nabla g}{\sqrt{\alpha^2 + |\nabla h^e - \nabla g|^2}} \right) + \mu(h^e - y) = 0 \qquad \text{in } Q, \tag{4.11}$$

the Neumann boundary condition (4.10) on $\partial\Omega$, where h_α is replaced by h^e, and the initial condition $h^e(0) = h_0$.

It can be shown that the solution of a discretized time dependent problem at an instant t converges to the solution of the discretized stationary problem as t tends to infinity.

The calculations have been performed for the case that Ω is a rectangular domain. The above nonstationary problems for u^e and h^e were solved by finite difference method using explicit schemes, both in time and space. For the spatial discretization, a staggered grid has been chosen, with each vertex of the grid at points at which the noisy intensity y is given.

Below we omit the superscript e in the notations of the unknown functions. We use the standard forward/backward difference operators $D_{x_1}^{\pm}$ and $D_{x_2}^{\pm}$, and the centered difference operators C_{x_1} and C_{x_2} in the x_1 and x_2 directions respectively.

We first determine the tangential vector $\mathbf{v}$ as $(v_1, v_2)^T = (-D_{x_2}^- y, D_{x_1}^- y)^T$. Starting with the initial values $u_1^0 = v_1, u_2^0 = v_2$ and $\lambda^0 = 0$, the values of u_1, u_2 and λ at step $n+1$ are calculated as follows:

$$\frac{u_1^{n+1} - u_1^n}{\Delta t} = D_{x_1}^- \left(\frac{D_{x_1}^+ u_1^n}{T_1^n} \right) + D_{x_2}^- \left(\frac{D_{x_2}^+ u_1^n}{T_2^n} \right) - \delta\,(u_1^n - v_1) + D_{x_1}^- \lambda^n, \tag{4.12}$$

$$\frac{u_2^{n+1} - u_2^n}{\Delta t} = D_{x_1}^- \left(\frac{D_{x_1}^+ u_2^n}{T_2^n} \right) + D_{x_2}^- \left(\frac{D_{x_2}^+ u_2^n}{T_1^n} \right) - \delta\,(u_2^n - v_2) + D_{x_2}^- \lambda^n, \tag{4.13}$$

$$\frac{\lambda^{n+1} - \lambda^n}{\Delta t} = \frac{1}{\epsilon} \left(D_{x_1}^+ u_1^n + D_{x_2}^+ u_2^n \right), \tag{4.14}$$

where

$$T_1^n = \sqrt{\left(A_{x_2}(C_{x_1}u_1^n)\right)^2 + \left(D_{x_2}^+ u_1^n\right)^2 + \alpha^2}, \tag{4.15}$$

$$T_2^n = \sqrt{\left(D_{x_2}^+ u_2^n\right)^2 + \left(A_{x_2}(C_{x_1}u_2^n)\right)^2 + \alpha^2}, \tag{4.16}$$

and A_{x_1}, A_{x_2} are average operators, $(A_{x_1}w)(x_1,x_2) = \left(w(x_1,x_2) + w(x_1+\Delta x_1, x_2)\right)/2$ and $(A_{x_2}w)(x_1,x_2) = \left(w(x_1,x_2) + w(x_1,x_2+\Delta x_2)\right)/2$.

The function ∇g at the discrete formulation is defined as $\nabla g = (-u_2^{n_0}, u_1^{n_0})$, where n_0 is a large positive integer, and the image reconstruction step (4.11) takes the following form:

$$\frac{h^{n+1}-h^n}{\Delta t} = D_{x_1}^- \left(\frac{D_{x_1}^+ h^n + u_2^{n_0}}{T_3^n}\right) + D_{x_2}^- \left(\frac{D_{x_2}^+ h^n - u_1^{n_0}}{T_4^n}\right) - \mu\left(h^n - y\right), \tag{4.17}$$

where T_3 and T_4 are defined as

$$T_3 = \sqrt{\left(D_{x_1}^+ h^n + u_2^{n_0}\right)^2 + \left(A_{x_1}(C_{x_2}h^n) - u_1^{n_0}\right)^2 + \alpha^2},$$

$$T_4 = \sqrt{\left(D_{x_2}^+ h^n - u_1^{n_0}\right)^2 + \left(A_{x_2}(C_{x_1}h^n) + u_2^{n_0}\right)^2 + \alpha^2}.$$

Although the applied numerical methods provide the convergence of approximate solutions to the exact ones, they are of course not the best. It seems likely that the methods of augmented Lagrangian with a saddle-point approach, that is used for solution of the minimization problem with pointwise restriction $\operatorname{div} u = 0$ in [4] is more effective for the problem (3.12), and the dual algorithm of [10] is more effective for problem (3.25).

5. Numerical Examples. We have used the modified TV-Stokes model for denoising a number of images; some of those results are presented in this section. We consider the case that $y = h + \eta$, where h is the true image and η is a random noise with the noise level $\sigma = \|\eta\|_{L^2(\Omega)} = \|h - y\|_{L^2(\Omega)}$. The signal to noise ratio (SNR) is measured as the number in decibels,

$$SNR = 20 \cdot \log_{10}\left(\frac{\int_\Omega (h-\overline{h})^2\,dx}{\int_\Omega (\eta-\overline{\eta})^2\,dx}\right), \tag{5.1}$$

where

$$\overline{h} = \frac{1}{|\Omega|}\int_\Omega h\,dx \quad \text{and} \quad \overline{\eta} = \frac{1}{|\Omega|}\int_\Omega \eta\,dx \tag{5.2}$$

are the averages of h and η, respectively, $|\Omega| = \int_\Omega dx$.

Experiments show that the modified TV-Stokes model, as well as the original TV-Stokes model [33], give smooth images that are visually very pleasant, especially in smooth areas of an image. At places where the texture changes very rapidly, the modified TV-Stokes model seems to smear out the image and thereby loose some of the fine scale details. However, this is the most common drawback of many image processing models based on variational methods.

Below we present results of calculations for images with gray level values in the range between 0 (black) and 1 (white). In all our experiments, we expose our image to random noise with zero mean. The value of α^2 was 10^{-10} in the first step in (3.10),

and 10^{-12} in the second step in (3.34). In the first step, the iteration stops when the corresponding energy value converges at least up to one decimal point, and the discrete L_2-norm of the divergence falls below 0.5×10^{-1}. In the second step, the iteration stops when the corresponding energy value and the computed noise level converge up to their second decimal points.

The quality of the resulting image depends on the choice of the parameters δ and μ. Smaller δ results in higher smoothing of the tangential field, and, consequently, the image. Conversely, a larger δ results in less smoothing. After δ has been fixed, we use μ for the fine tuning.

Calculations were performed for several models and results of calculations for the modified TV-Stokes model are compared with results for other models. Results of calculations are illustrated in figures 5.1-5.6. In each figure we show an original image and the noisy and the denoised images corresponding to different models. The difference images, included in figures 5.1-5.5, demonstrate the difference between the noisy image and the corresponding denoised image for the modified TV-Stokes model. The SNR values of the noisy and the denoised images are also given in these figures.

In our first example we apply the modified TV-Stokes model to the Ali image with smooth surfaces, cf. Figure 5.1. A random noise with noise-level ≈ 25.94 has been added to the image. As we can see from the figure, the modified TV-Stokes model performs quite well in preserving edges as well as in reproducing smooth surfaces. The time steps used for the smoothing and reconstruction steps were 0.5×10^{-4} and 0.5×10^{-3}, respectively. Both parameters δ and μ were 12. For the ROF model we set $\mu = 12$ and the time step was 0.5×10^{-3}. The contour plots clearly reveal that the modified TV-Stokes model, as compared to the ROF model, generates images with smoother surfaces and with smooth and uniformly separated level lines, especially visible around the nose, the eye balls, and the lips.

Same tests were performed in our second example, see Fig 5.2, where we consider denoising of the Barbara image with noise level ≈ 11.09. In this case $\delta = 30$ and $\mu = 40$, and the corresponding time-steps were 0.1×10^{-4} and 0.1×10^{-3} respectively. For the ROF model $\mu = 30$ and the time step was 0.1×10^{-3}. The original image contains both texture parts and smooth parts, and they are quite well preserved in the denoised image. Contour plots show that the modified TV-Stokes model gives smooth surfaces and uniformly separated smooth level lines. The ROF model fails to reproduce the smooth surfaces, it approximates the surface with a function that is close to a step function.

Three more images, where the modified TV-Stokes have been applied, are presented in Figures 5.3-5.5. These images have significant features like thin fiber textures or weak signals. In all cases the modified TV-Stokes model performs well in representing these features in the resulting images.

The image of Baboon, see Fig. 5.3, has thin fiber textures. and random noise 15.03. For this image $\delta = 17$, $\mu = 15$, and the corresponding time steps were 0.1×10^{-4} and 0.1×10^{-2} respectively. Due to the fibrous structure, this image poses a difficult challenge to most models. For a moderate noise the modified TV-Stokes model performs quite well, especially in capturing the structure.

In Figure 5.4, we display our results for the satellite image with noise-level ≈ 22.68. In this case $\delta = 10$, $\mu = 17$, and the corresponding time-steps were 0.2×10^{-4} and 0.1×10^{-3}, respectively. In Figure 5.5, we display our results for the Cameraman image with noise-level ≈ 14.52. In this case $\delta = 16$, $\mu = 18$, and the corresponding time-steps were 0.1×10^{-4} and 0.5×10^{-3}, respectively. Both images have thin structures

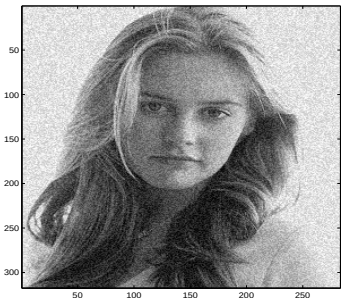

(a) Noisy image, SNR≈28.03

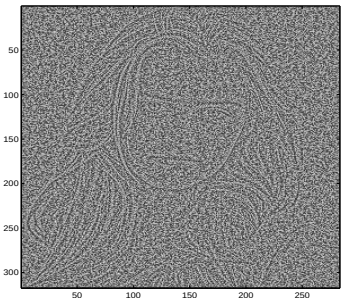

(b) TV-Stokes Difference image

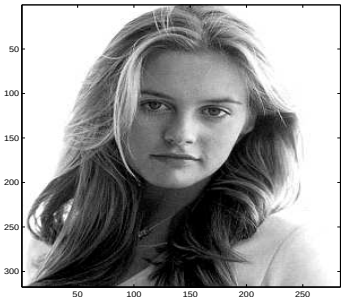

(c) Original image

(d) Contour, original image

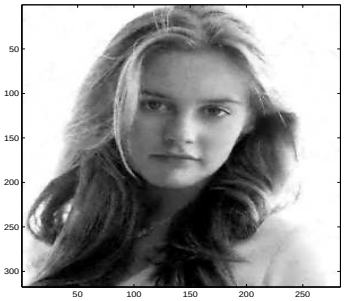

(e) TV-Stokes denoised, SNR≈43.8

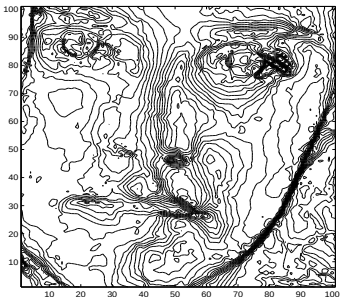

(f) Contour, TV-Stokes image

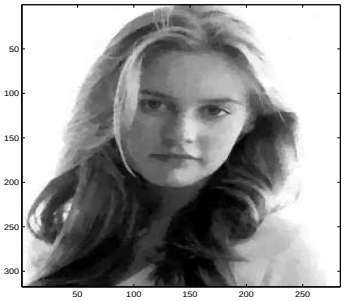

(g) ROF denoised, SNR≈42.3

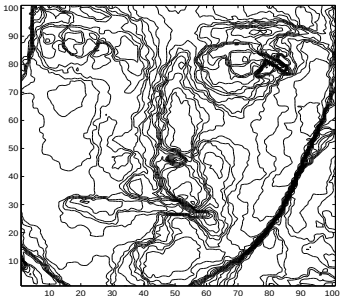

(h) Contour, ROF image

FIG. 5.1. *The Ali image (317×283), denoised using the modified TV-Stokes and the ROF algorithm. Zoomed-in contour plots are shown.*

(a) Noisy image, SNR≈32.3

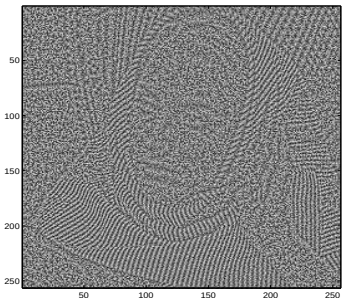

(b) TV-Stokes difference image

(c) Original image

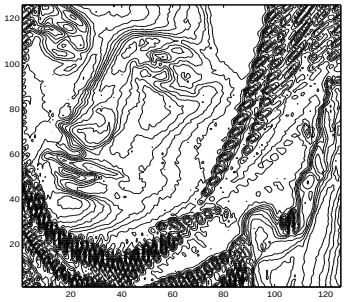

(d) Contour, original image

(e) TV-Stokes denoised, SNR≈40.7

(f) Contour, TV-Stokes image

(g) ROF denoised, SNR≈37.2

(h) Contour, ROF image

FIG. 5.2. *The Barbara image (256×256), denoised using the modified TV-Stokes and the ROF algorithm. Zoomed-in contour plots are shown.*

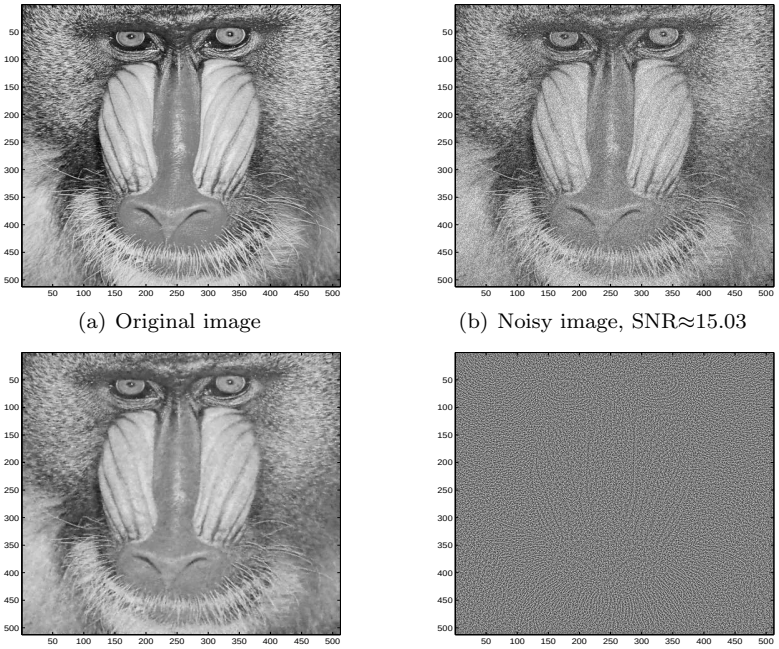

(a) Original image (b) Noisy image, SNR≈15.03

(c) TV-Stokes denoised, SNR≈22.2 (d) TV-Stokes difference image

FIG. 5.3. *The Baboon image (512×512), denoised using the modified TV-Stokes algorithm.*

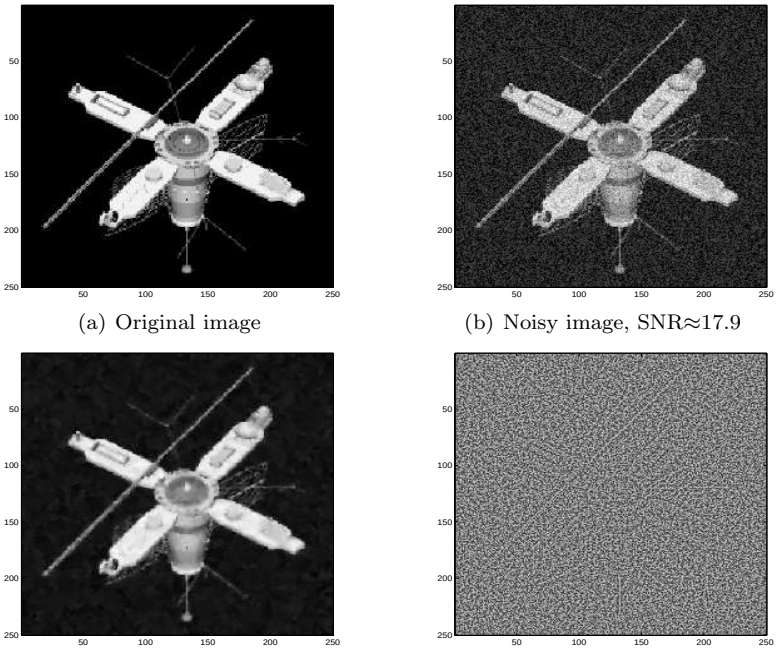

(a) Original image (b) Noisy image, SNR≈17.9

(c) TV-Stokes denoised, SNR≈23.8 (d) TV-Stokes difference image

FIG. 5.4. *The Satellite image (250×250), denoised using the modified TV-Stokes algorithm.*

and weak signals. Again, for moderate noise the modified TV-Stokes captures the thin structures and the weak signals quite well.

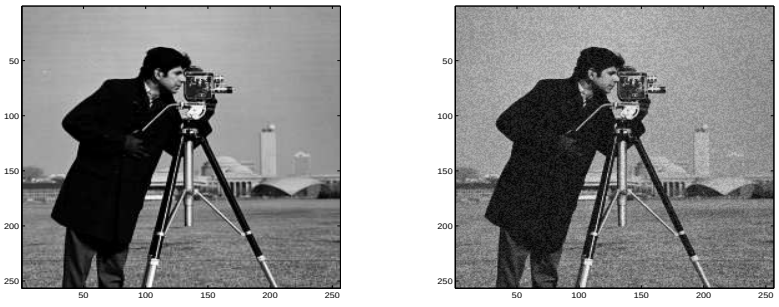

(a) Original image (b) Noisy image, SNR≈29.7

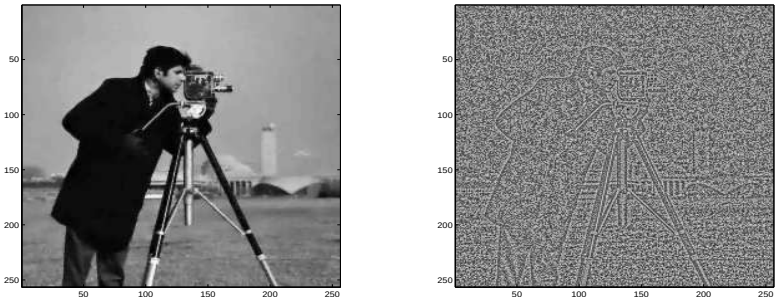

(c) TV-Stokes denoised, SNR≈40.1 (d) TV-Stokes difference image

FIG. 5.5. *The Cameraman image (256×256), denoised using the modified TV-Stokes algorithm.*

Finally, we compare the modified TV-Stokes model with a few other models on the Lena image, cf. Figure 5.6. This includes the second order ROF model, the fourth order LLT model [27], and the two-step LOT model [28]. A comparison of calculations for these models can be found in the paper [28]. We have used the same noisy image as it was in that paper. The images 5.6(a)- 5.6(e) are taken directly from the paper [28]. The image 5.6(f) is the denoised image for the modified TV-Stokes model. The ROF model demonstrates the staircase effect. It is known that the LOT model preserves edges quite well, but it is seen from the figure, it cannot get rid of the staircase effect. The other models, namely, the fourth order model and the modified TV-Stokes model result in smoother surfaces in the smooth regions of the image. The fourth order model, however, has produced patches of black cloud. The modified TV-Stokes model has produced an image which is visually more pleasant than all the other models shown here.

Now we present some examples of application of the modified TV-Stokes model to image inpainting. In these examples, we consider the domain B as a domain surrounding the inpainting region. By using the above algorithms, we have solved the problem (3.12) in the first step and the problem (3.35) in the second step.

In our first experiment, cf. Figure 5.7, we consider an old photo which had been damaged. The damaged area has been masked with white color, cf. Figure 5.7(a), representing our inpainting region Ω_I. The modified TV-Stokes model has been applied to this image, and the repaired image is shown in Figure 5.7(b).

In our next experiment, we consider two images, whose surface plots in three

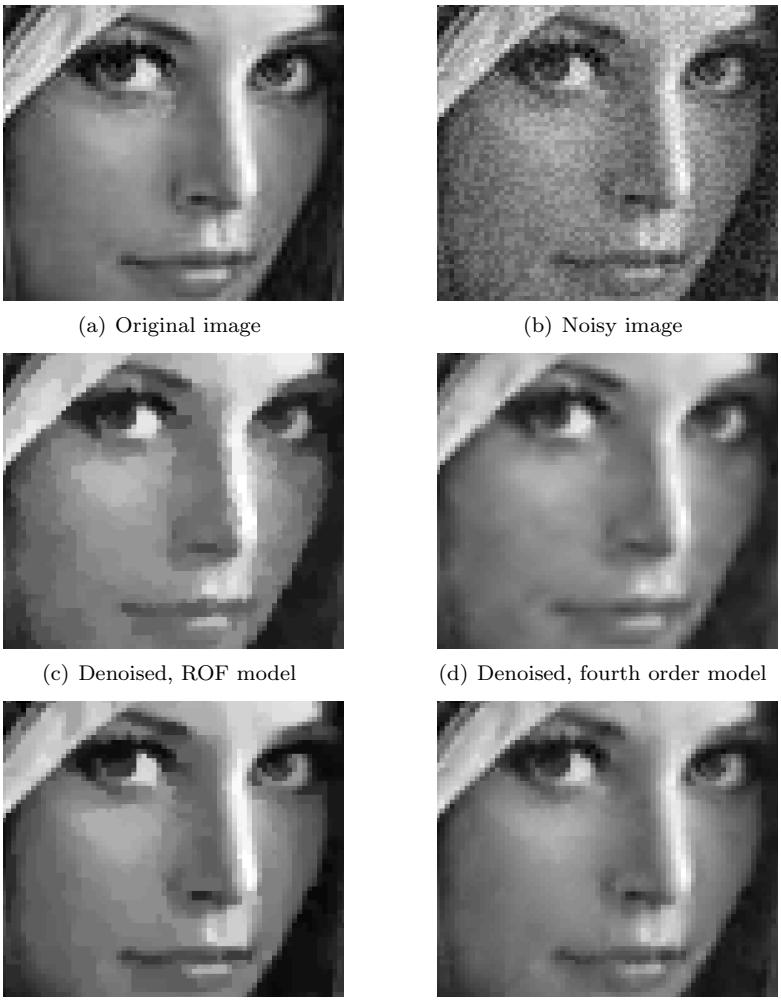

(a) Original image (b) Noisy image

(c) Denoised, ROF model (d) Denoised, fourth order model

(e) Denoised, LOT model (f) Denoised, modified TV-Stokes

FIG. 5.6. *Comparisons of different models on the Lena image (100×100). Images (a)-(e) are taken from [28].*

(a) Damaged photo (b) Repaired photo

FIG. 5.7. *Repairing a damaged photo (405×483) through image inpainting.*

(a) 2D pyramid image with inpainting region

(b) 2D cone image with inpainting region

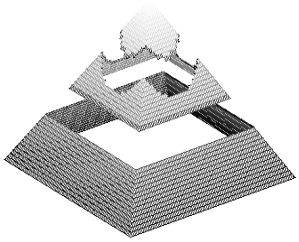

(c) Surface plot of pyramid image

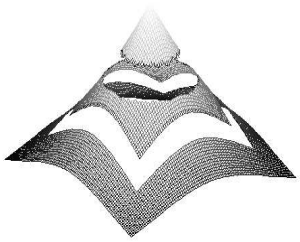

(d) Surface plot of cone image

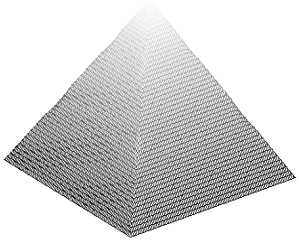

(e) Pyramid image inpainted

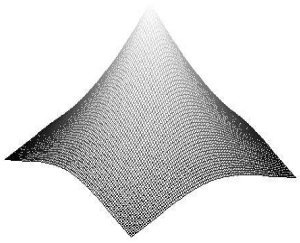

(f) Cone image inpainted

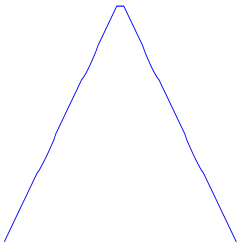

(g) Intensity along a diagonal of inpainted pyramid

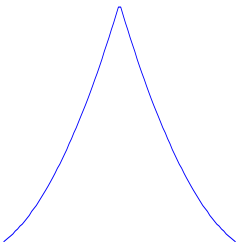

(h) Intensity along a diagonal of inpainted cone

FIG. 5.8. *Inpainting of a pyramid and a cone image (100×100).*

dimensions are a pyramid (left figures in Fig. 5.8) and a cone (right figures in Fig 5.8). The projections of both images on the plane have rectangular and circular band inpainting regions (see the first row in the Fig. 5.8 and confer it with the second one). The inpainted images are shown in the third row. The difficult parts for inpainting in these images are the ones that are along the diagonals. The corresponding plots of intensity along the diagonals are shown in the last row of the Fig. 5.8.

One can see from these figures that the modified TV-Stokes model effects a good inpainting in the case of the cone and a quite good inpainting in the case of the pyramid. It follows from the all the above figures that the modified TV-Stokes model produces comparatively good results in image denoising and quite good results in image inpainting.

REFERENCES

[1] L. Ambrosio, N Fusco, and D. Pallara, *Functions of bounded variation and free discontinuity problems.* The Caledron Press Oxford University Press, New York, 2000.

[2] R. Acar, C. R. Vogel, *Analysis of bounded variation penalty methods for ill-posed problems*, Inverse Problems, Vol. 10, pp. 1217-1229, 1994.

[3] G. Aubert and P. Kornprobst, *Mathematical Problems in Image Processing: Partial Differential Equations and the Calculus of Variations*, Applied Mathematical Sciences 147, 2002, Springer Verlag, New York.

[4] M.S. Belonosov and W.G. Litvinov, *Finite element method for nonlinearly viscous fluids*, Z. Angew. Math. Mech. Vol. 76, 1996, pp. 307–320.

[5] C. Ballaster, M. Bertalmio, V. Caselles, G. Sapiro, and J. Verdera, *Filling in by Joint Interpolation of Vector Fields and Gray Levels*, IEEE Trans. Image Processing, No. 10, 2000, pp. 1200–1211.

[6] M. Bertalmio, A. L. Bertozzi, and G. Sapiro, *Navier-Stokes, Fluid Dynamics and Image and Video Inpainting*, In Proc. Conf. Comp. Vision Pattern Rec., 2001, pp. 355–362.

[7] P. Blomgren, and T. Chan, *Color TV: Total variation methods for restoration of vector-valued images*, IEEE Trans. Image Processing, Vol. 7, No. 3, pp. 304–309, 1998.

[8] A. Buades, B. Coll, and J. M. Morel, *A review of image denoising algorithms, with a new one*, Multiscale Model. Simul., Vol. 4, 2005, No. 2, pp. 490-530.

[9] P. Burchard, T. Tasdizen, R. Whitaker, and S. Osher, *Geometric Surface Processing via Normal Maps*, Tech. Rep. 02-3, Applied Mathematics, 2002, UCLA.

[10] A. Chambolle, *An algorithm for total variation minimization and applications*, J. Math. Imaging. Vis., Vol. 20, 2004, pp. 89-97.

[11] T. F. Chan, J. Shen, H. M. Zhou, *Total variation wavelet inpainting*, J. Math. Imaging Vision, Vol. 25, No.1, pp. 107-125, 2006.

[12] T. F. Chan, H. M. Zhou, , *Total variation wavelet thresholding*, J. Sci. Comput., Vol. 32, pp. No. 2, 315-341, 2007.

[13] P. Ciarlet, *Finite Element Method for Elliptic Problems*, North-Holland Publishing Company, Amsterdam, 1978.

[14] A. Chambolle and P..L Lions, *Image recovery via total variation minimization and related problems*, Numerische Mathematik, Vol. 76, No. 3, pp. 167–188, 1997.

[15] T.F. Chan and J. Shen, *Image Processing and Analysis: Variational, PDE, Wavelet, and Stochastic Methods*, 2005, SIAM, Philadelphia.

[16] T.F. Chan, A. Marquina, and P. Mullet, *High-order total variation-based image restoration*, Siam J. Scientific Computing, Vol. 22, No. 2, pp. 503–516, 2000.

[17] M. Fornaiser, R. march, *Restoration of color images by vector valued BV functions and variational calculus*, Submitted, 2006.

[18] V. Girault and P.A. Raviart, *Finite Element Approximation of the Navier-Stokes Equations*, Springer, 1981.

[19] Enrico Giusti, *Minimal Surfaces and Functions of Bounded Variation.* Monographs in Mathematics, Vol.80, A.Borel, J. Moser and S.-T. Yau, eds., Birkhäuser, 1984.

[20] R. Glowinski and P. LeTallec, *Augmented Lagrangian and Operator-Splitting Methods in Nonlinear Mechanics*, SIAM Studies in Applied Mathematics, Vol. 9, 1989, SIAM, Philadelphia.

[21] S.H. Kang, and R. March, *Variational models for image colorization via chromatic and brightness decomposition*, Submitted, 2006.

[22] C. Kenny, and J. Langan, *A new image processing primitive: reconstructing images from modified flow fields*, University of California Santa Barbara Preprint, 1999.

[23] S. Kindermann, S. Osher, and J. Xu, *Denoising by BV-duality*, J. Sci. Comput., Vol. 28, Sept. 2006, pp. 414–444.

[24] D. Krishnan, P. Lin, and X.C. Tai, *An Efficient Operator-Splitting Method for Noise Removal in Images*, Commun. Comput. Phys., Vol. 1, 2006, pp. 847–858.

[25] W. G. Litvinov, *Optimization in Elliptic Problems with Applications to Mechanics of Deformable Bodies and Fluid Mechanics.* Monographs in Mathematics, Birkhäuser, 2000.

[26] Q. Liu, Z. Yao, and Y. Ke, *Entropy solutions for a fourth-order nonlinear degenerate problem for noise removal*, Nonlinear Analysis, Vol. 67, pp. 1908–1918, 2007.

[27] A. Lundervold, M. Lysaker, and X.C. Tai, *Noise removal using fourth-order partial differential equation with applications to medical magnetic resonance images in space and time*, Tech. Rep. 02-44, UCLA, Applied Mathematics, 2002.

[28] M. Lysaker, S. Osher, and X.C. Tai, *Noise Removal Using Smoothed Normals and Surface Fitting*, IEEE Trans. Image Processing, Vol. 13, No. 10, October 2004, pp. 1345–1357.

[29] T. Lu, P. Neittaanmaki and X-C Tai, *A parallel splitting up method and its application to Navier-Stokes equations*, RAIRO Math. Model. and Numer. Anal., Vol. 26, No.6, pp. 673–708, 1992.

[30] T. Lu, P. Neittaanmaki and X-C Tai, *A parallel splitting up method and its application to Navier-Stokes equations*, Applied Mathematics Letters, Vol. 4, No. 2, pp.25-29, 1991.

[31] S. Osher, A. Sole, and L. Vese, *Image Decomposition and Restoration Using Total Variation Minimization and the H^{-1} norm*, Multiscale Modelling and Simulation, A SIAM Interdisciplinary J., Vol. 1, No. 3, 2003, pp. 1579–1590.

[32] L.I. Rudin, S. Osher, and E. Fatemi, *Nonlinear Total Variation Based Noise Removal Algorithms*, Physica D., Vol. 60, 1992, pp. 259–268.

[33] T. Rahman, X.C. Tai, and S. Osher, *A TV-Stokes denoising algorithm*, Lecture Notes in Computer Science, 4485, F. Sgallari, et al. eds., pp. 473–483, Springer Verlag, 2007.

[34] C. Shannon, W. Weaver, *The mathematical Theory of Communication*, University of Illinois Press, Champaign, IL, 1998.

[35] X.C. Tai, S. Osher, and R. Holm, *Image Inpainting using TV-Stokes equation*, in: Image Processing based on partial differential equations, 2006, Springer, Heidelberg.

[36] L. Vese and S. Osher, *Numerical Methods for P-Harmonic Flows and Applications to Image Processing*, SIAM J. Numer. Anal., Vol. 40, No. 6, December 2002, pp. 2085–2104.

[37] Y.-L. You, and M. Kaveh, *Fourth-order partial differential equation for noise removal*, IEEE Trans. Image Processing, Vol. 09, No. 10, pp. 1723–1730, 2000.